Electronic Supplementary Material (ESI) for Journal of Materials Chemistry A.
This journal is © The Royal Society of Chemistry 2019

Supporting information

Self-supported copper-based gas diffusion electrodes for CO_2 electrochemical reduction

Jie Zhang [a,b], Wen Luo [a,b] *, and Andreas Züttel [a,b]

[a] Laboratory of Materials for Renewable Energy (LMER), Institute of Chemical Sciences and Engineering (ISIC), Basic Science Faculty (SB), École Polytechnique Fedérale de Lausanne (EPFL) Valais/Wallis, Energypolis, Rue de l'Industrie 17, CH-1951 Sion, Switzerland

[b]Empa Materials Science & Technology, CH-8600 Dübendorf, Switzerland

*Corresponding email: wen.luo@epfl.ch

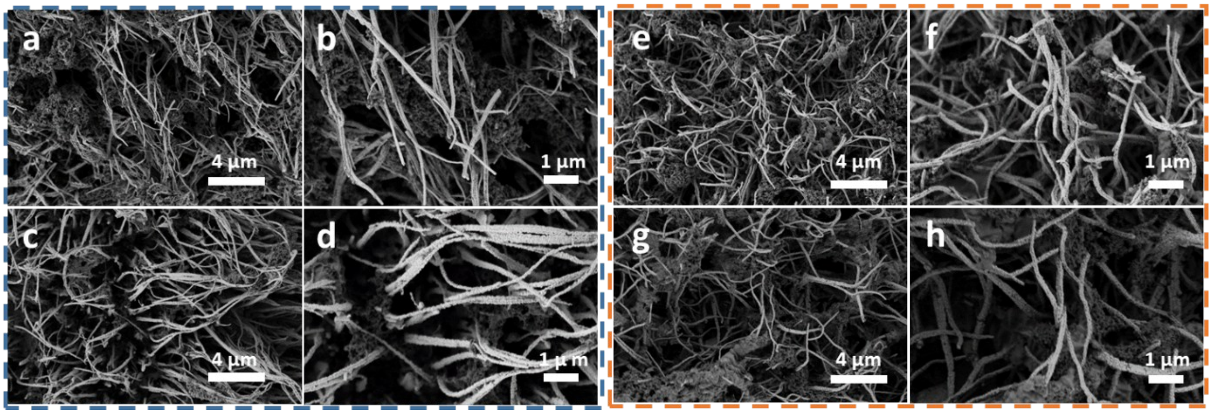

Figure S1 SEM images of the TA-Cu and WCO-Cu based GDE just-reduced and after 6 h of CO_2RR in flow cell with 1 M KOH. (a, b) TA-Cu based GDE after electrochemical reduction, (c, d) TA-Cu based GDE after 6 h of reaction. (e, f) WCO-Cu based GDE after electrochemical reduction, (g, h) WCO-Cu based GDE after 6 h of reaction.

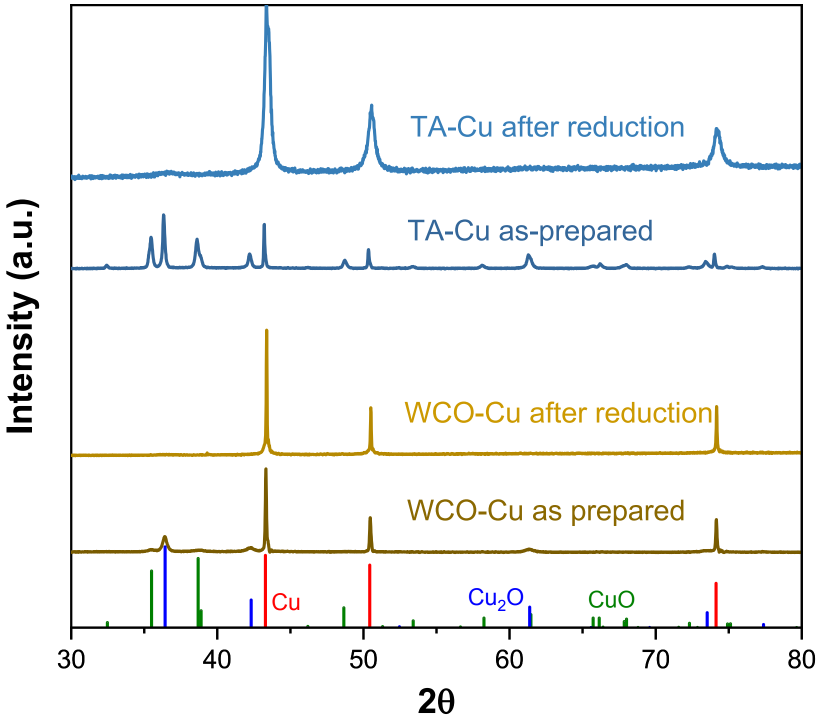

Figure S2 XRD patterns of TA-Cu and WCO-Cu before and after being electrochemically reduced in H-cell.

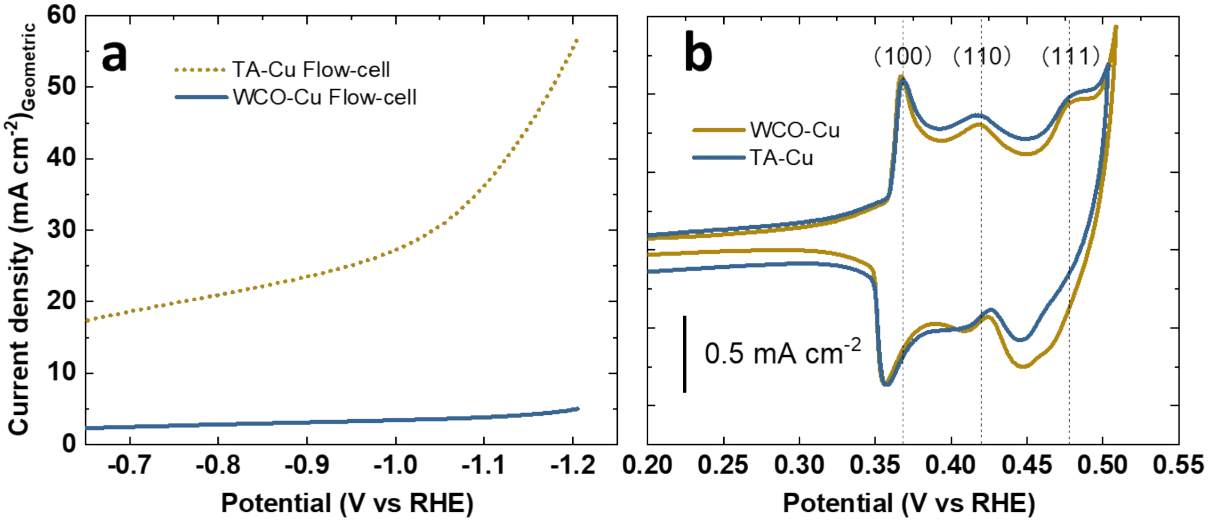

Figure S3 (a) Voltammograms of the WCO-Cu and TA-Cu based GDEs in flow cell with Ar saturated 1.0 M KOH at a scan rate of 50 mV/s. (b) Voltammograms of OH_{ads} peaks on the WCO-Cu and TA-Cu collected in H-cell with Ar saturated 1.0 M KOH at a scan rate of 10 mV/s.

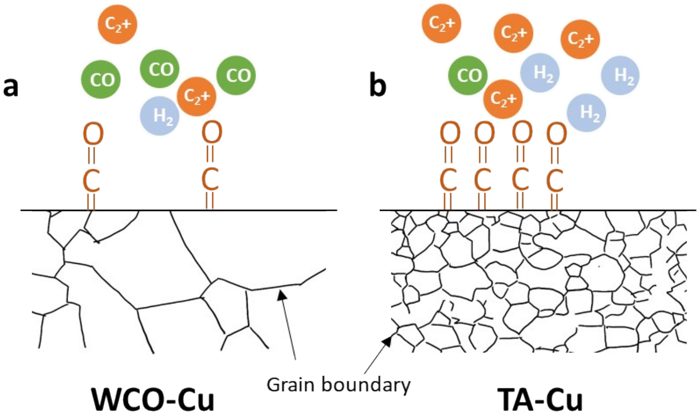

Figure S4 Schematics of the effect of the density of grain boundary on the adsorption of *CO intermediate and the formation of the CO, H_2 and C_{2+} products. (a) WCO-Cu with smaller density of grain boundary, (b) TA-Cu with denser grain boundary.

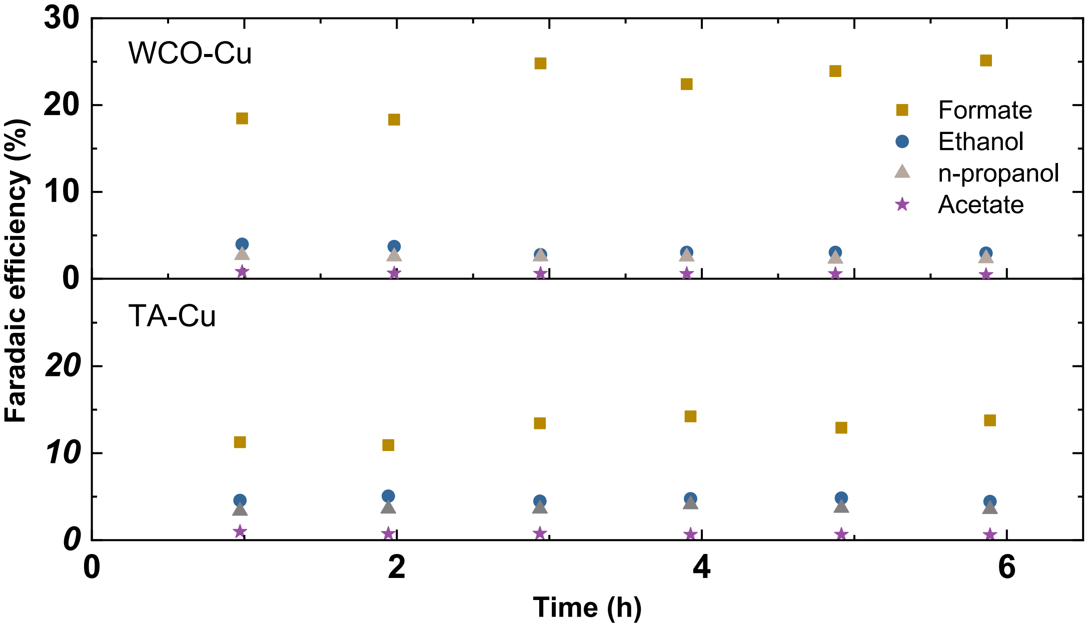

Figure S5 Faradaic efficiency of the liquid products as a function of time from the CO_2RR on the TA-Cu and WCO-Cu based GDEs in 1.0 M KOH.

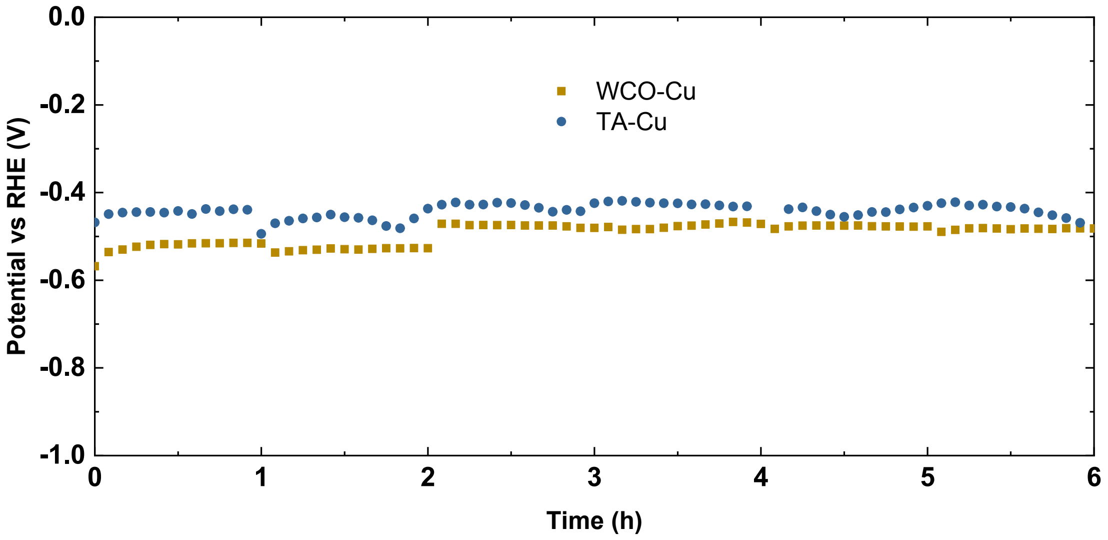

Figure S6 Potential versus time for the TA-Cu and WCO-Cu based GDEs in 1.0 M KOH. WCO-Cu electrode was measured at 100 mA cm^{-2} and TA-Cu electrode at 150 mA cm^{-2}.

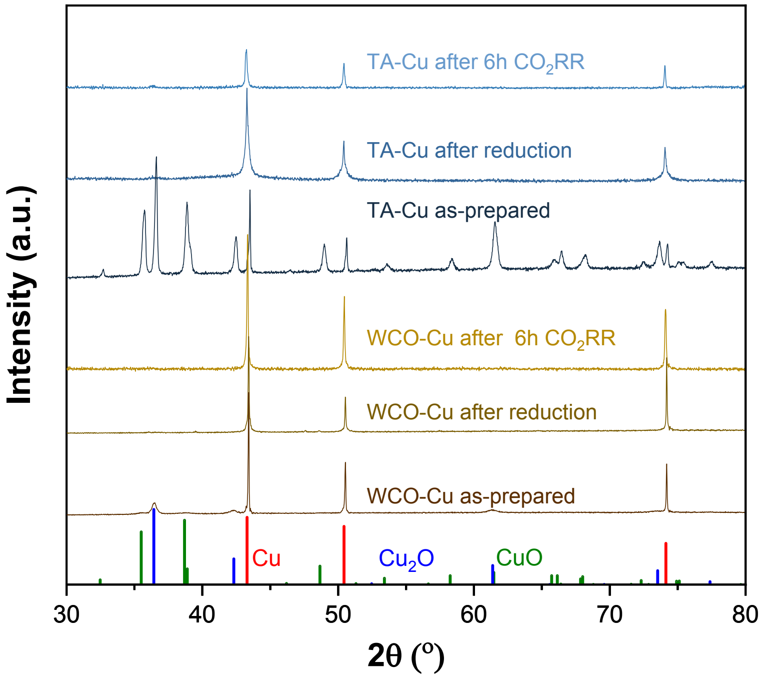

Figure S7 XRD patterns of the as-prepared TA-Cu and WCO-Cu based GDEs and those after reduction and 6 h of CO_2RR in flow-cell with 1 M KOH.

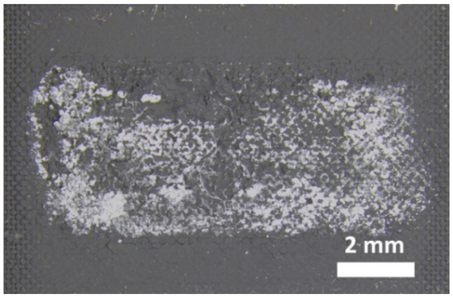

Figure S8 The accumulated salt on the gas diffusion side of TA-Cu based GDE after continuously working for 1 h at 150 mA cm^{-2} in flow cell using 1 M KOH as the electrolyte.

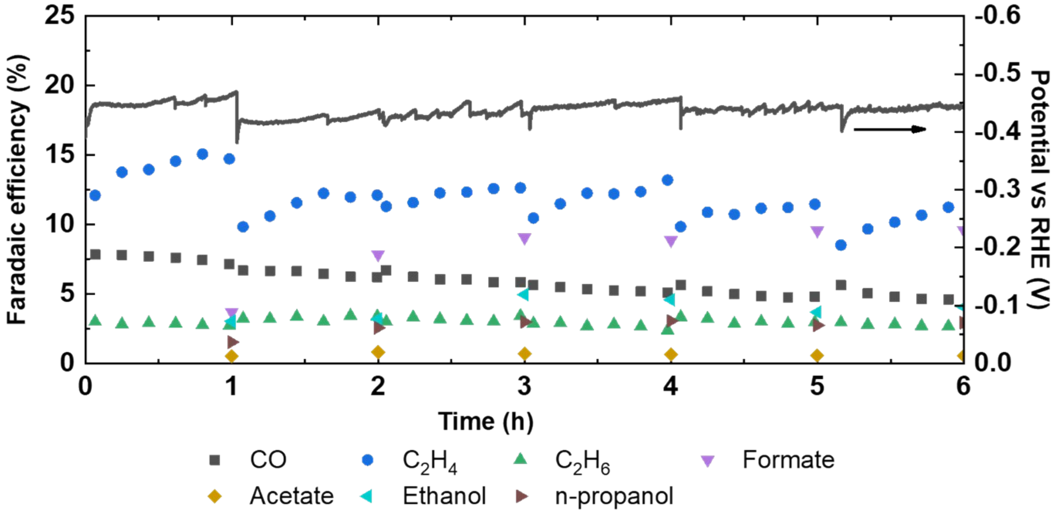

Figure S9 FEs and potential as the function of time of a TA-Cu GDE working for 6 h at 100 mA cm^{-2} in flow cell with 1 M KOH as the electrolyte. The electrode was rinsed by water every hour.

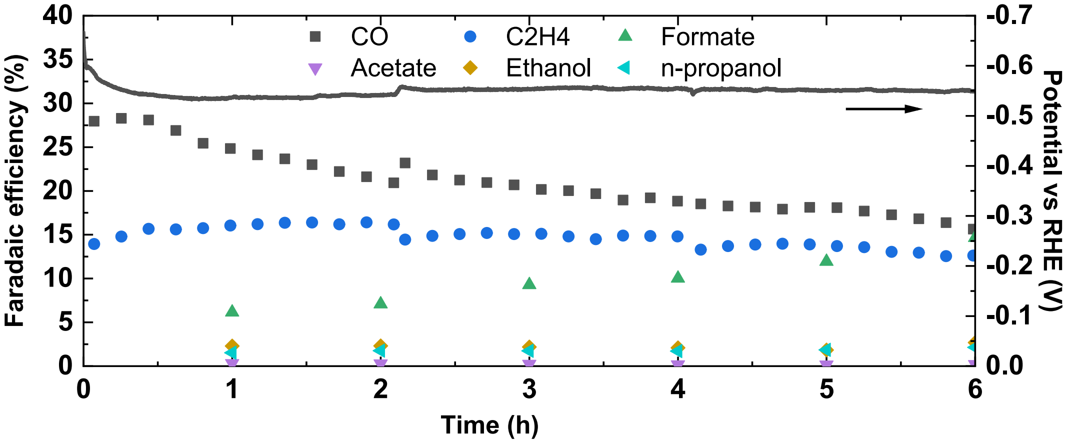

Figure S10 FEs and potential as the function of time of a WCO-Cu GDE continuously working for 6 h at 100 mA cm^{-2} in flow cell with 1 M KOH as the electrolyte.

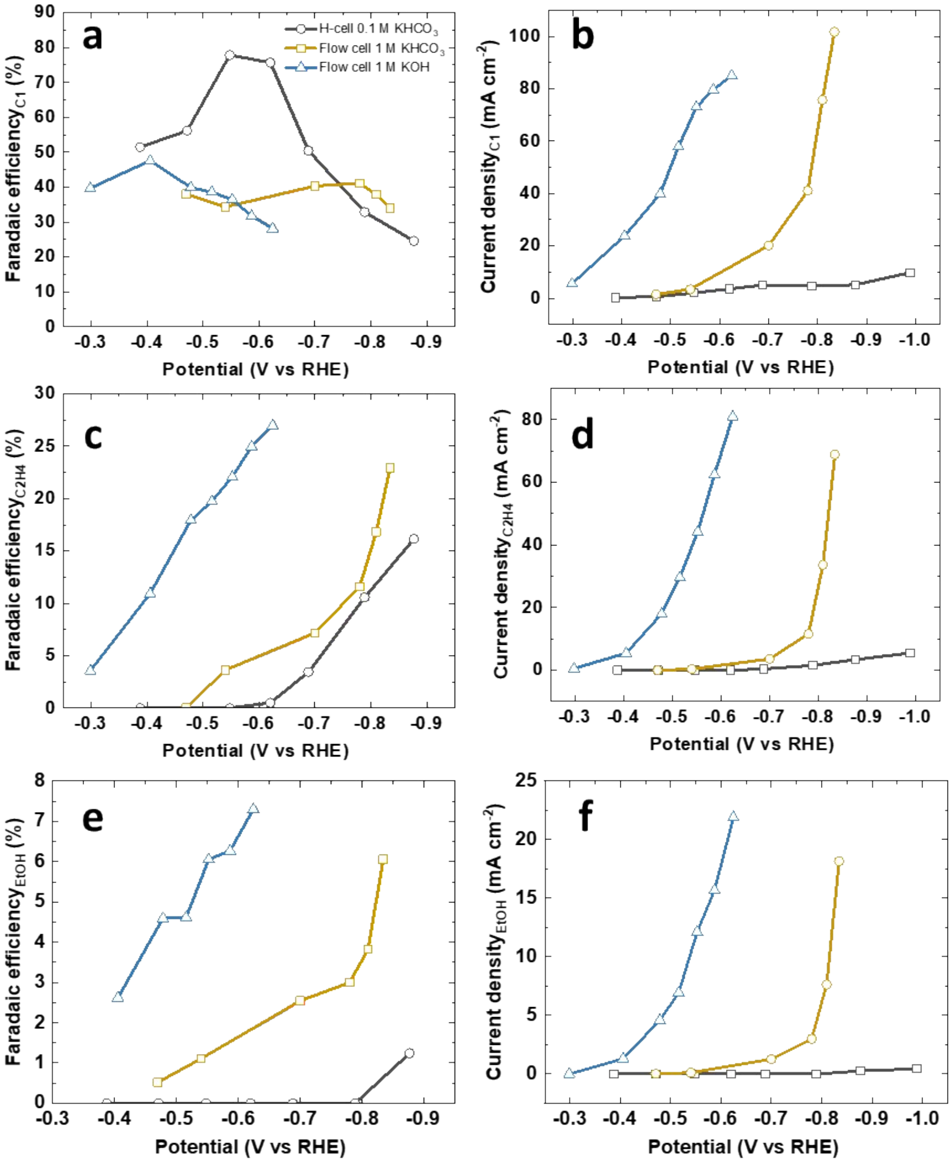

Figure S11 Faradaic efficiency (a, c, e) and partial current density (b, d, f) as a function of potential for C_1 products, C_2H_4, and ethanol, respectively, generated on the WCO-Cu catalysts in a flow cell with 1 M KOH or 1 M $KHCO_3$ and H-cell with 0.1 M $KHCO_3$.

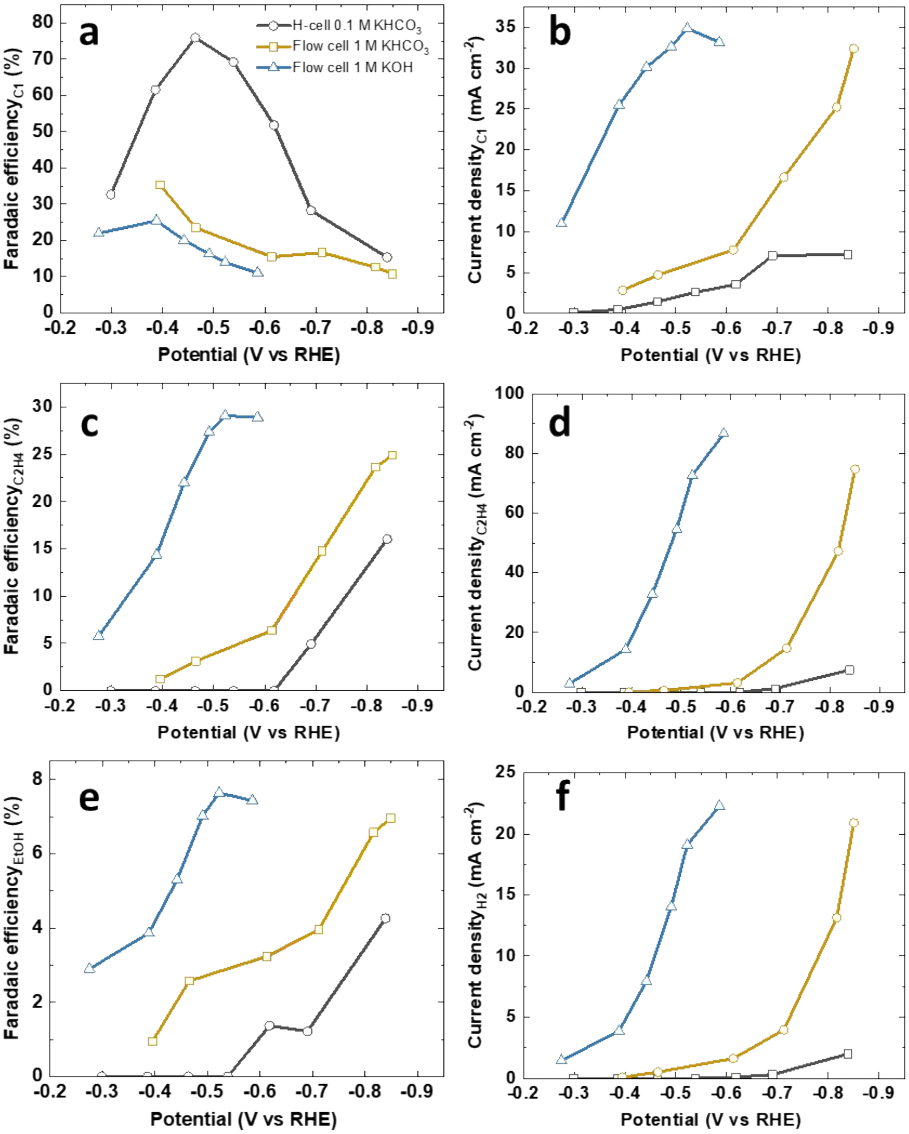

Figure S12 Faradaic efficiency (a, c, e) and partial current density (b, d, f) as a function of potential for C_1 products, C_2H_4, and ethanol, respectively, generated on the TA-Cu catalysts in a flow cell with 1 M KOH or 1 M $KHCO_3$ and H-cell with 0.1 M $KHCO_3$.

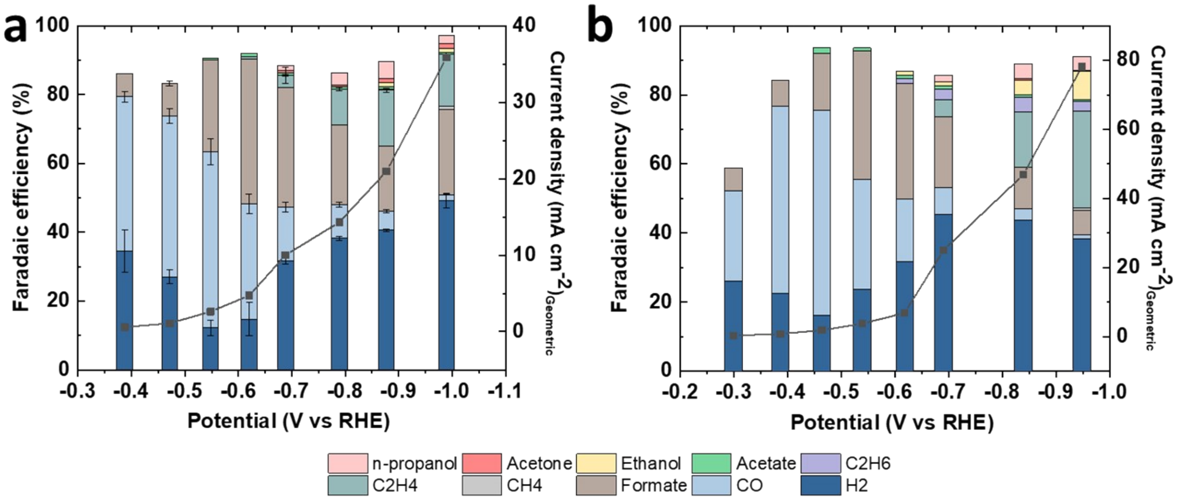

Figure S13 Faradaic efficiency and current density as the function of potential of all the detected products from CO_2RR on (a) WCO-Cu and (b) TA-Cu in H-cell reactor using 0.1 M $KHCO_3$.

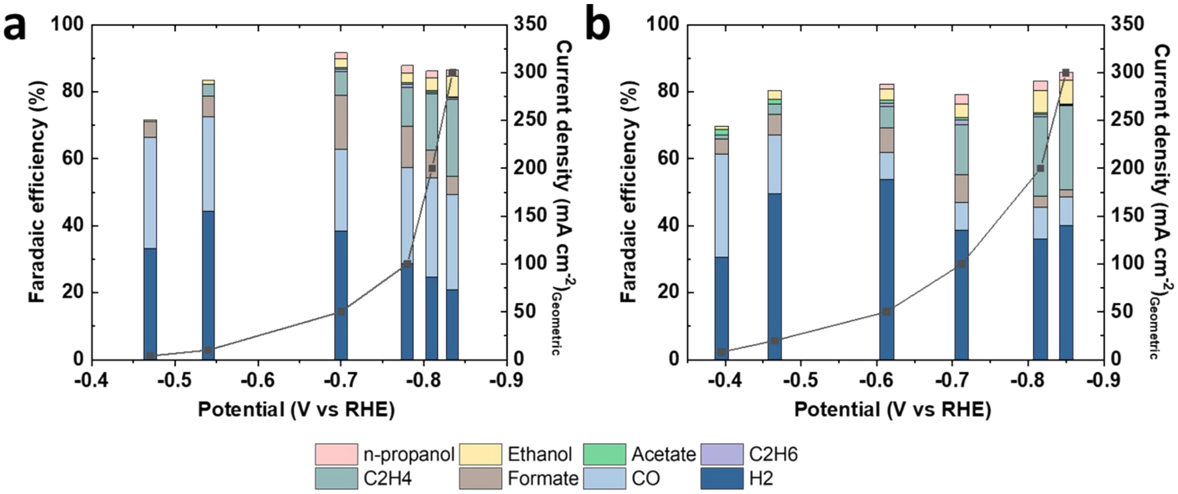

Figure S14 Faradaic efficiency and current density as the function of potential of all the detected products from CO_2RR on (a) WCO-Cu GDEs and (b) TA-Cu GDEs in flow with 1 M $KHCO_3$.

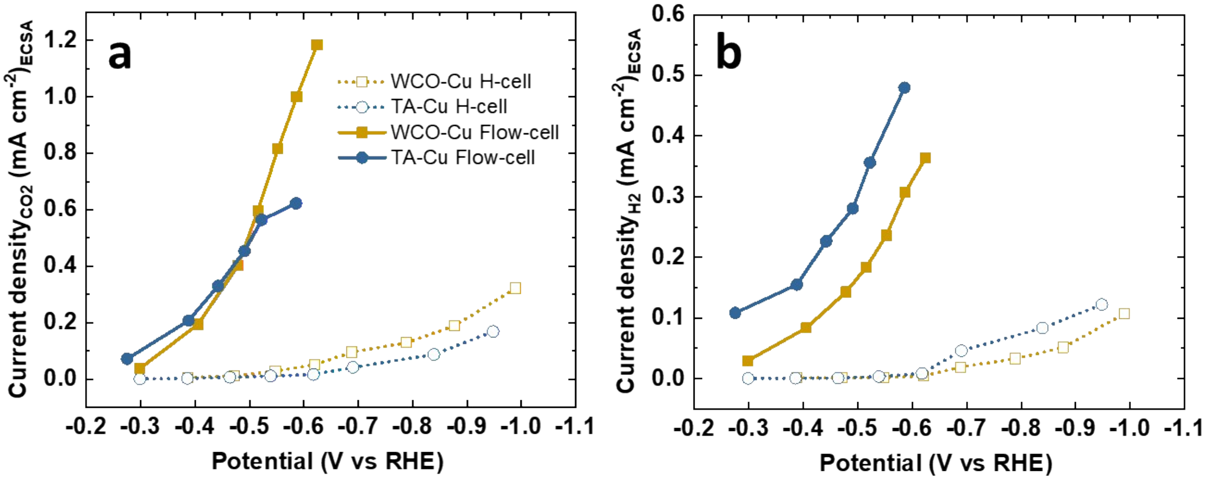

Figure S15 Comparison of CO_2RR (a) and HER (b) activity between WCO-Cu and TA-Cu in both flow cell and H-cell. The current density was normalized by the electrochemical active surface area derived from the roughness factor from Figure S16. The Flow cell has 1 M KOH as the electrolyte and the H-cell has 0.1 M $KHCO_3$ as the electrolyte.

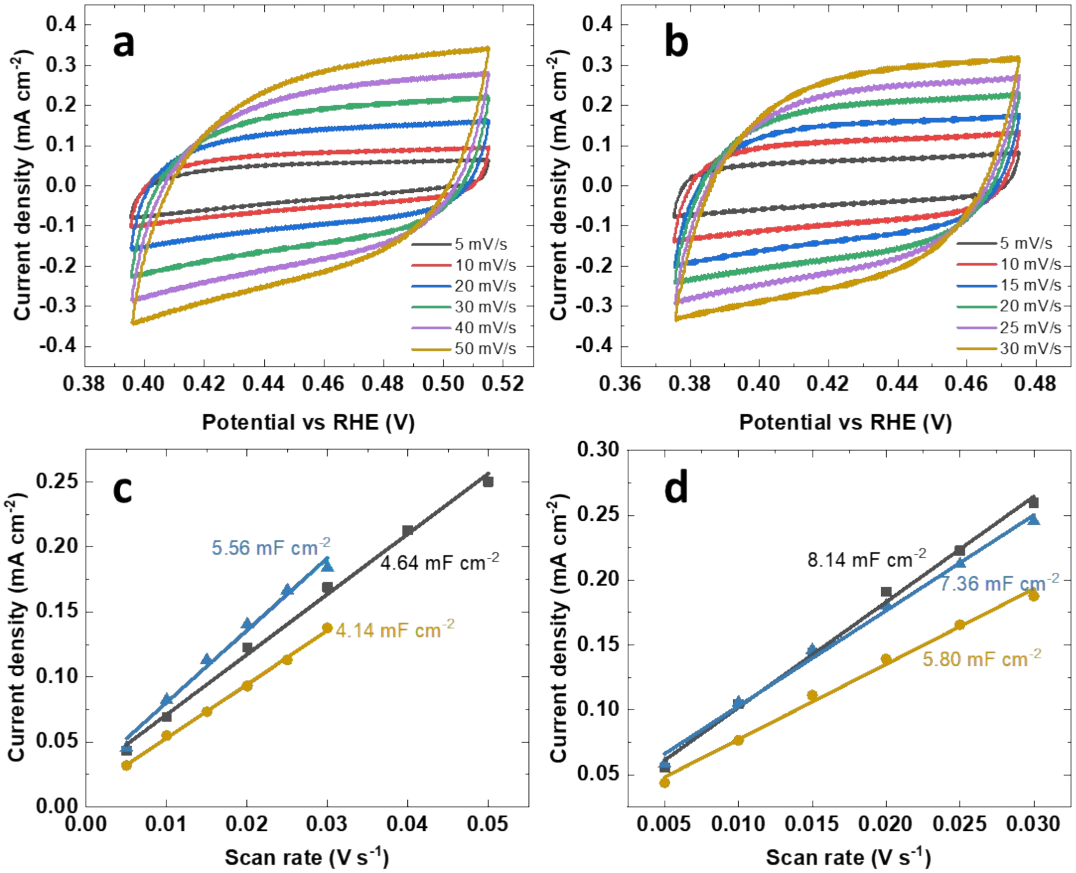

Figure S16 Determination of the double layer capacitance of the WCO-Cu and TA-Cu. Cyclic voltammograms of (a) WCO-Cu and (b) TA-Cu at various scan rate in a potential window where only double layer charging and discharging are involved. The plots of corresponding current density against CV scan rate on (C) WCO-Cu and (d) TA-Cu. For each catalyst, the CVs measurements were repeated on three independent samples.

Table S1 Capacitance values and surface roughness factors derived from the CVs corresponding to Figure S15. The surface roughness factor of polycrystalline Cu is from Ref 1 [1] and defined as 1.

Electrode	Capacitance	Surface roughness factor
Polycrystalline Cu [1]	29 μF cm^{-2}	1
WCO-Cu	4.78 ± 0.59 mF cm^{-2}	165
TA-Cu	7.10 ± 0.97 mF cm^{-2}	245

Table S2 Faradaic efficiency and current density as the function of potential of WCO-Cu and TA-Cu in three conditions: H-cell with 0.1 M $KHCO_3$, flow cell with 1 M $KHCO_3$, and flow cell with 1 M KOH, corresponding to Figure S10 and S11, and Figure 3, respectively. The average values of at least three measurements were reported.

Potential	**Faradaic efficiency (%)**									**Current density**
V vs RHE	**H_2**	**CO**	**C_2H_4**	**C_2H_6**	**Formate**	**Acetate**	**Ethanol**	**Acetone**	**n-propanol**	mA cm^{-2}
WCO-Cu in H-cell with 0.1 M KHCO3										
-0.39	34.60	44.73			6.73					0.59
-0.47	27.02	46.74	0.00	0.00	9.45	0.00	0.00	0.00	0.00	1.08
-0.55	12.21	51.14	0.00	0.00	26.73	0.55	0.00	0.00	0.00	2.62
-0.62	14.77	33.45	0.49	0.00	42.23	1.01	0.00	0.00	0.00	4.72
-0.69	31.61	15.75	3.43	0.10	34.71	0.75	0.00	0.63	1.53	10.00
-0.79	38.22	9.71	10.56	0.00	23.11	0.76	0.00	0.39	3.63	14.32
-0.88	40.57	5.48	16.16	0.27	19.08	0.67	1.24	1.22	4.82	20.94
-0.99	49.26	1.66	15.24	0.00	24.64	0.31	1.25	1.49	2.19	35.88
TA-Cu in H-cell with 0.1 M KHCO3										
-0.30	26.15	25.99	0.00	0.00	6.68	0.00	0.00	0.00	0.00	0.31
-0.39	22.62	54.13	0.00	0.00	7.39	0.00	0.00	0.00	0.00	0.74
-0.46	16.07	59.40	0.00	0.00	16.54	1.69	0.00	0.00	0.00	1.85
-0.54	23.60	31.95	0.00	0.00	37.23	0.82	0.00	0.00	0.00	3.75
-0.62	31.61	18.18	0.00	1.25	33.60	0.88	1.37	0.00	0.00	6.88
-0.69	45.35	7.89	4.94	3.10	20.39	0.90	1.22	0.00	1.92	25.00
-0.84	43.73	3.30	16.02	4.08	12.08	0.75	4.26	0.57	4.25	46.88
-0.95	38.37	1.06	27.97	2.91	7.07	0.38	8.22	0.36	3.99	78.13
WCO-Cu in flow cell with 1 M $KHCO_3$										
-0.47	33.14	33.15			4.88		0.52			4.00
-0.54	44.28	28.29	3.63		6.05		1.11			10.00
-0.70	38.48	24.25	7.18	0.67	16.09	0.54	2.55		1.87	50.00
-0.78	28.61	28.64	11.60	0.87	12.46	0.43	3.00		2.22	100.00
-0.81	24.66	29.61	16.82	0.58	8.26	0.35	3.82		2.10	200.00
-0.83	20.81	28.48	22.95	0.53	5.45	0.24	6.06		1.94	300.00
TA-Cu in flow cell with 1 M $KHCO_3$										
-0.40	30.50	30.83	1.21		4.51	1.60	0.94			8.00
-0.47	49.63	17.41	3.12		6.09	1.53	2.57			20.00
-0.61	53.81	8.00	6.37	0.79	7.50	1.01	3.23		1.60	50.00
-0.71	38.64	8.25	14.78	1.52	8.41	0.67	3.96		2.88	100.00
-0.82	36.15	9.47	23.64	0.88	3.15	0.47	6.57		2.92	200.00
-0.85	40.00	8.58	24.92	0.29	2.22	0.33	6.96		2.39	300.00
WCO-Cu in flow cell with 1 M KOH										
-0.30	35.25	25.85	3.56		13.86					14.00
-0.41	27.63	24.93	10.93	0.51	22.66	0.26	2.62		2.07	50.00
-0.48	23.63	21.80	17.95	0.65	18.07	0.36	4.60		2.99	100.00
-0.52	20.23	23.91	19.73	0.30	14.65	0.22	4.61		2.28	150.00
-0.55	19.50	22.73	22.08	0.30	13.68	0.22	6.06		2.19	200.00
-0.59	20.28	21.09	24.98	0.39	10.64	0.25	6.27		2.26	250.00
-0.62	20.03	18.85	26.98	0.31	9.24	0.24	7.30		1.99	300.00
TA-Cu in flow cell with 1 M KOH										
-0.28	53.19	11.14	5.76	1.47	10.83	1.65	2.89		1.15	50.00
-0.39	37.99	9.16	14.36	2.79	16.32	1.29	3.86		2.84	100.00
-0.44	37.03	7.15	21.98	2.22	12.93	0.99	5.30		3.26	150.00
-0.49	34.36	6.60	27.34	1.13	9.71	0.69	7.02		3.06	200.00
-0.52	34.91	7.50	29.07	1.11	6.45	0.67	7.64		2.82	250.00
-0.59	39.17	6.11	28.90	0.62	4.95	0.47	7.43		2.37	300.00

References

1. C. W. Li and M. W. Kanan, *Journal of the American Chemical Society*, 2012, **134**, 7231-7234.